Reply to reviewer #1: Interactive comment on "Continuous online-monitoring of Ice Nucleating Particles: development of the automated Horizontal Ice Nucleation Chamber (HINC-Auto)" by Cyril Brunner and Zamin A. Kanji.

Reviewer comments are reproduced in **bold** and author responses in normal typeface; extracts from the original manuscript are presented in *red italic*, and from the revised manuscript in *blue italic*.

In this technical manuscript, the authors present a new instrument, HINC-Auto, allowing continuous measurements of INP concentrations at fixed temperature and humidity conditions. This instrument is based on the design of the HINC chamber with modifications brought in order to remove the need of a human operator. It is the first paper to report such instrument capable to measure INP concentration online in an automatic way for period that can extend several months. The scientific approach is well built and does not raise any of my concerns. Furthermore, this manuscript is well written and easy to follow. This manuscript is a very valuable source of technicality for the ice community I am in favor of publication after the authors have answer the few questions and recommendations listed below:

We would like to thank the reviewer for the compliments and valuable comments and address the comments individually below.

Line 18: "The interaction between aerosols and clouds contributes to the global energy budget by directly influencing the radiative forcing of the climate system." should read:
"The interaction between aerosols and clouds contributes to the global energy budget by indirectly influencing the radiative forcing of the climate system."

A critical error, thank you! We agree with the reviewer, and changed the sentence as proposed (see line 18 revised manuscript):

The interaction between aerosols and clouds contributes to the global energy budget by indirectly influencing the radiative forcing of the climate system.

Line 66: Presently, no automated online INP counter is available (Cziczo et al., 2017; Lacher et al., 2017). A novel paper has just been submitted to AMTD, several weeks after the present one, showing another automatic online INP counter (expansion type chamber): https://amt.copernicus.org/preprints/amt-2020-307/

We agree with the reviewer, and now include reference to this paper. We correspondingly altered Line 64 (revised manuscript) as stated below. In addition, we learned from the work by Bi et al., 2019, https://doi.org/10.1029/2019JD030609, in which they presented a continuous online INP counter.

A prime limitation for the absence of long term monitoring data sets was that online real-time measurements of INP concentrations via INP counters required human operators as no autonomous online INP counter were available. Bi et al. (2019) presented the first autonomous online INP counter based on a CFDC. A novel paper by Möhler et al. (2020) introduced the Portable Ice Nucleation Experiment (PINE), an autonomous online INP counter that uses the adiabatic cooling during expansion to activate the INPs at the targeted supersaturation.

Line 92: "The surrounding sheath air is dried and filtered before entering the chamber.
missing "dried"

We agree with the reviewer, and changed line 94 (revised manuscript) as proposed:

The surrounding sheath air is dried and filtered before entering the chamber.

Line 121: "A polyvinylidene fluoride (PVDF) spacer physically and thermally separates the two chamber walls."

We agree with the reviewer, and changed line 123 (revised manuscript) as proposed:

A polyvinylidene fluoride (PVDF) spacer physically and thermally separates the two chamber walls.

Figure 3: Red and Green is a bad color combination as it is the most common form of colorblindness.

We agree with the reviewer, and changed Figure 3 such that color is no longer required to read it:

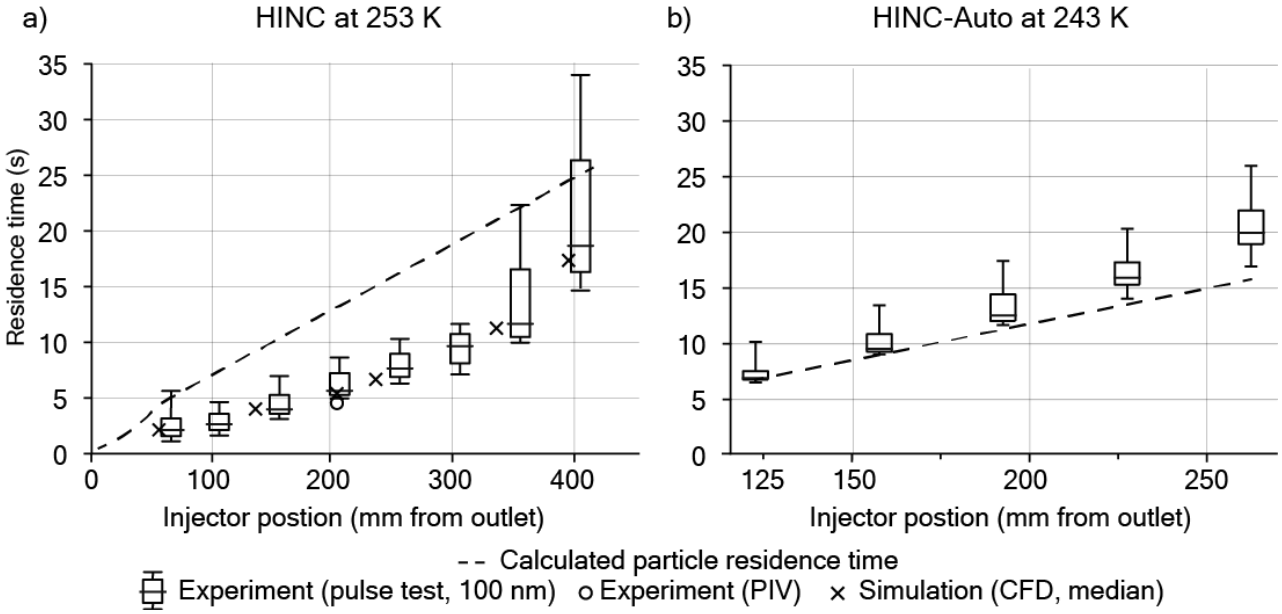

Figure 3.

Figure 3a: How thick is the ice layer and is it included in the calculations (solid line)? The ice layer might decrease the actual volume of the chamber, increase the flow velocity and thus decrease the residence time of particles.

This is a valid statement. The filter paper is 0.5 mm think, if fully soaked with water and frozen 0.6 mm. This translates to a chamber height of 18.8 mm for a freshly replenished ice layers and 19 mm for depleted ice layers. The flow velocity of the center lamina increases by 1.1 % from 19.33 mm/s to 19.54 m/s. We attribute this change to be minor in light of the uncertainty in lamina thickness, S_w and T of the chamber.

Figure 3: It is confusing. If I understood correctly, the message here is that "To smooth the flow field within the chamber and achieve a more consistent desired unidirectional flow field, a mesh was introduced 20 mm downstream of the sheath air injector holes."
For clarity, maybe the legend of Figure 3 could be changed to: "Figure 3. Calculated and measured particle residence time in a) HINC (without mesh) for different injector positions at T = 253 K and b) HINC-Auto (using a mesh to make the flow more laminar) at T= 243 K. Box plots from pulse experiments: median with 25/75% quartiles, whiskers: 5/95% quantiles. Median of PIV experiment (circles, T = 288 K) and CFD simulation (crosses, T = 243 K)." or maybe comparing HINC auto with and without mesh would be more relevant?

We agree with the reviewer, and changed the figure caption of Figure 3 as followed:

Figure 3. Calculated and measured particle residence time in a) HINC (without mesh) for different injector positions at T = 253 K and b) HINC-Auto (using a mesh to achieve a more uniform flow) at T = 243 K. Box plots from pulse experiments: median with 25/75% quartiles, whiskers: 5/95% quantiles. Median of PIV experiment (circles, T = 288 K) and CFD simulation (crosses, T = 243 K).

Figure 4:- "residence time until outlet" is not very intuitive for this figure. I would suggest replacing it by "residence time after entering the chamber" and reverse the time scale. In that way, it is simpler to compare both chamber. The main message here being the effect of cooler temperature entering the chamber, not the total length of the chamber. That way it is easier for the reader to read, that with cooler air, it needs only 20 cm and xx second to reach equilibrium, compare to 30 cm in yy second at warmer sheath air temperature.

Also for a and b legend: I suggest to put temperature first as it is the reason, and length second as it is the consequence. a) T sheath air=298K, (original length, maybe not needed) b)Tsheath air=248 K, (10 cm shorter, maybe not needed)

We agree with the reviewer, and changed the figure legend, time axis scale, and caption of Figure 4 as follows:

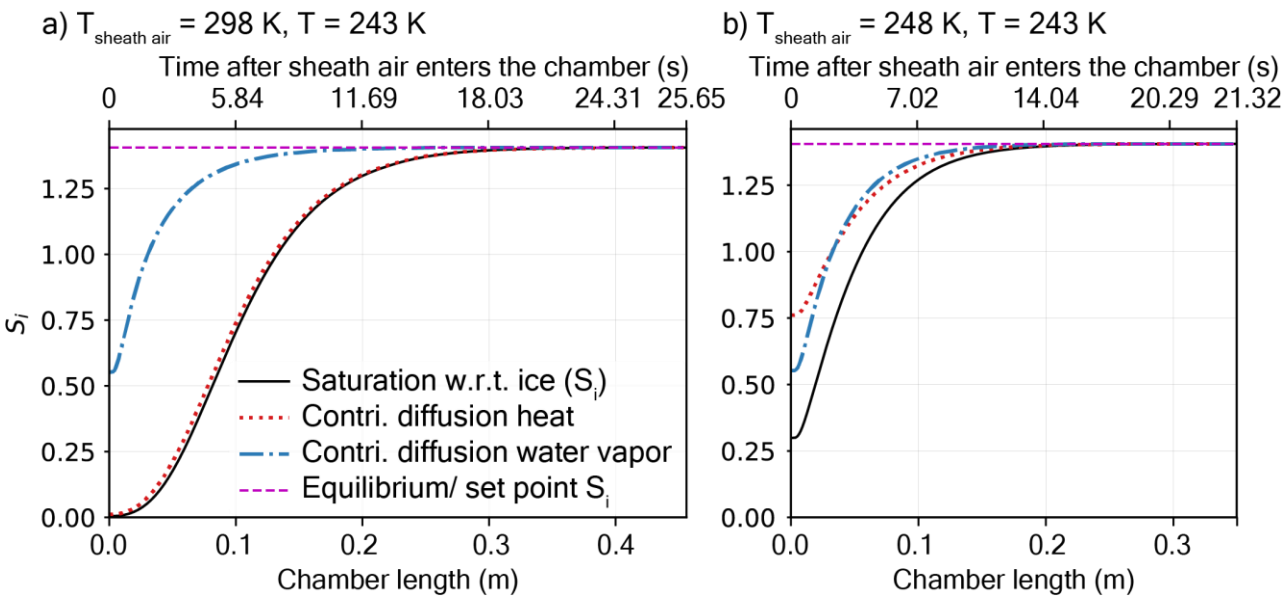

Figure 4. Simulated ice supersaturation development along the chamber's center lamina at T = 243 K and contributing factors diffusion of heat and water vapor for a) $T_{sheath\ air}$ = 298 K (original length) and b) $T_{sheath\ air}$ = 248 K (allowing for the chamber length to be reduced by 10 cm).

Line 210: "The chamber is controlled via a newly developed guided user interface programmed using Python 3.7 and corresponding open source packages. The postprocessing of INP concentrations is done in real time. HINC-Auto can be accessed and controlled remotely if a internet connection is available on site." A suggestion to the authors is to add in the appendix, a screen shot of the software interface could be presented, together with basic parameter that can be set by the user (RH ramping, Temperature profile,. . .).

We agree with the reviewer, and changed the paragraph as follows:

The chamber is controlled via a newly developed guided user interface programmed using Python 3.7 and corresponding open source packages. The postprocessing of INP concentrations is done in real time. HINC-Auto can be accessed and controlled remotely if an internet connection is available on site, however this is

not a requirement for autonomous operation. A screenshot of the guided user interface with comments on the basic parameters a user can set is shown in the appendix (A7-A10).

We further added the following subsection to the appendix:

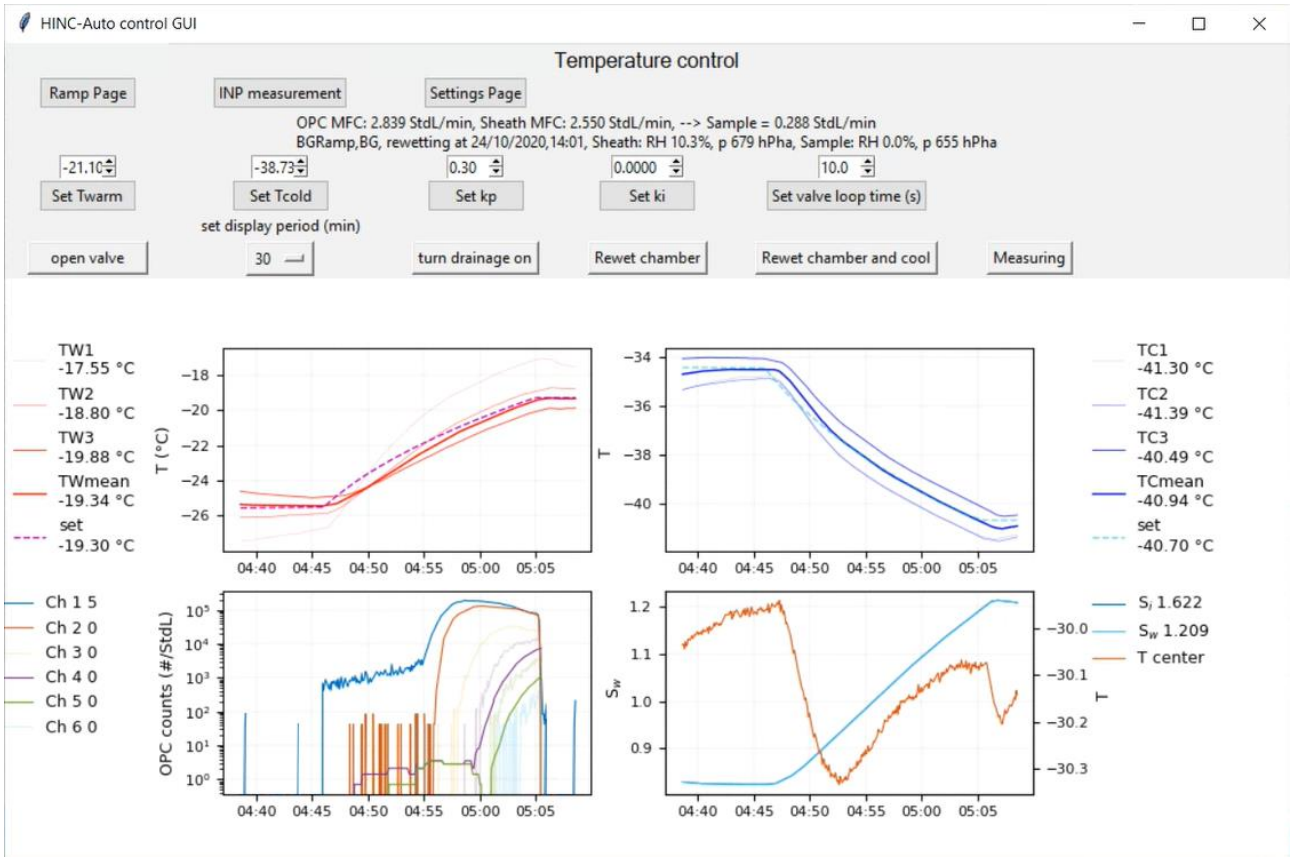

*Figure A8. Main window of the guided user interface used to control HINC-Auto. Top row buttons: **Ramp Page** leads to the window to run S_w- or T-ramps (see Figure A9). **INP measurement** leads to the window to run INP measurements (see Figure A10) and **Settings Page** leads to the window to change additional settings (see Figure A11). **OPC MFC** shows the current flow rate of the OPC mass flow controller (MFC), as reported by the MFC, **Sheath MFC** analogously shows the flow rate of the sheath flow MFC, **Sample** reports the difference between both MFC, which corresponds to the current sample flow rate. **BGRamp** shows the target state of the chamber, in this case "measuring the background after or before a RH- or T-ramp, **BG** shows the state in which the chamber currently is, **rewetting at** indicates the time of the next planned rewetting procedure (UTC), **Sheath** indicates the RH and pressure p of the sheath air as it enters the chamber (measured at mid-height within the chamber upstream of the mesh, thus at the same temperature as the chamber is set to) and **Sample** indicates the RH and pressure p of the sample air (just downstream of the sample diffusion dryer. Center row buttons: **Set Twarm** sets the target temperature of the warm wall, **Set Tcold** sets the target temperature of the cold wall, **Set kp** and **Set ki** set the proportional gain (k_p) and integral gain (k_i) of the PI-controller to control the warm wall temperature, **Set valve loop time (s)** defines the duration of a loop to actuate the warm wall solenoid valve. Bottom row buttons: **open valve** manually opens and closes the warm wall solenoid valve, **Set display period (min)** defines the amount of historic data to be shown in the four graphs below, **turn drainage on** manually actuates the pump to drain the chamber during rewetting, **Rewet chamber** executes the rewetting procedure, **Rewet chamber and cool** executes the rewetting procedure and cools the chamber back down to the set temperature of the chamber before the button was activated, **Measuring** changes the chamber's state and valves to sampling or background measurement. The top left graph shows the warm wall temperature (all three thermocouples, the computed mean wall temperature and the set temperature). The top right graph shows the cold wall temperature (all three thermocouples, the computed mean wall temperature and the set temperature). The bottom left graph shows the counts reported by the OPC for each of the six size-bins/ channels (here CH 1 set to ≥0.3*

µm, CH 2 set to ≥1 µm, CH 3 set to ≥3 µm, CH 4 set to ≥4 µm, CH 5 set to ≥5 µm, CH 6 set to ≥6 µm). The bottom right graph shows S_w and T for the center lamina (calculated).

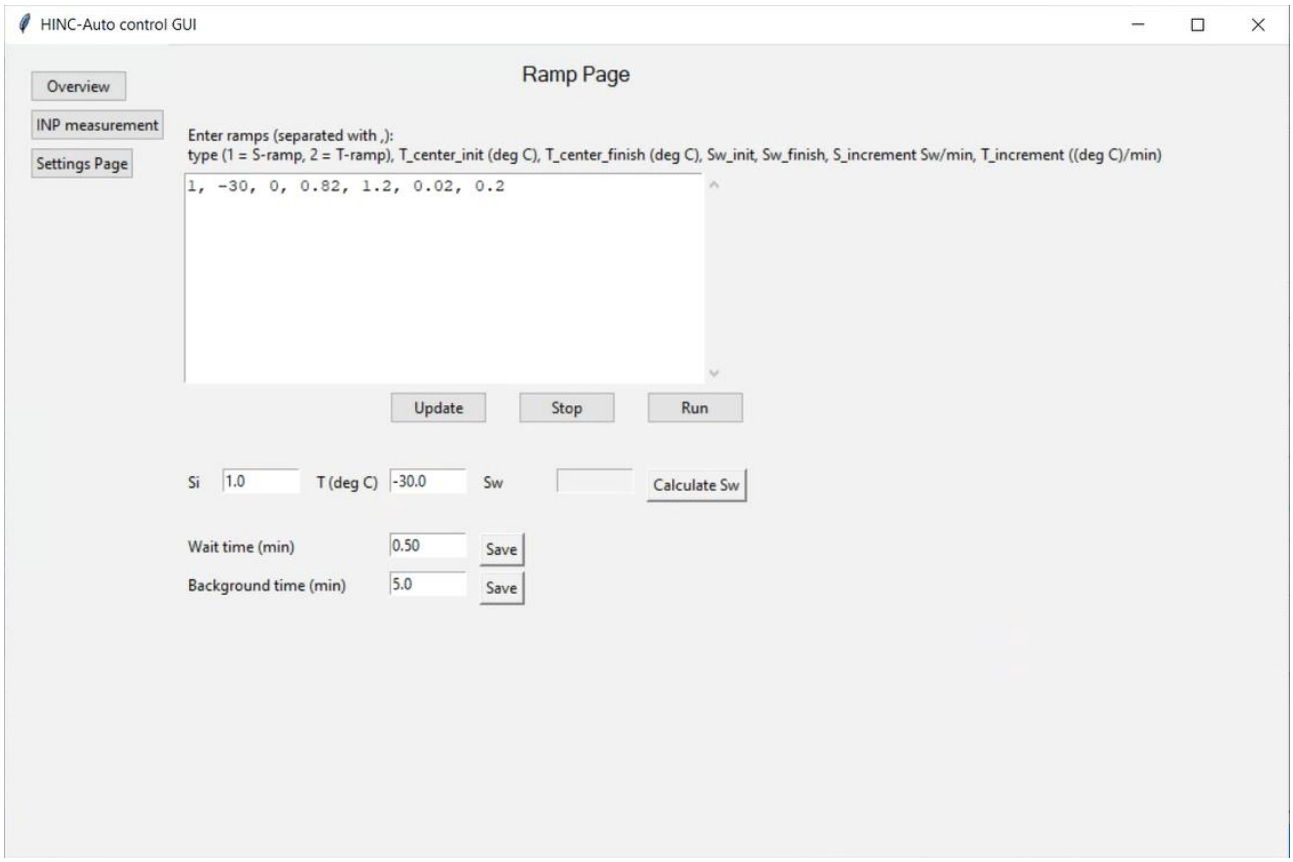

Figure A9. Window of the guided user interface used to control S_w - or T-ramps with HINC-Auto.

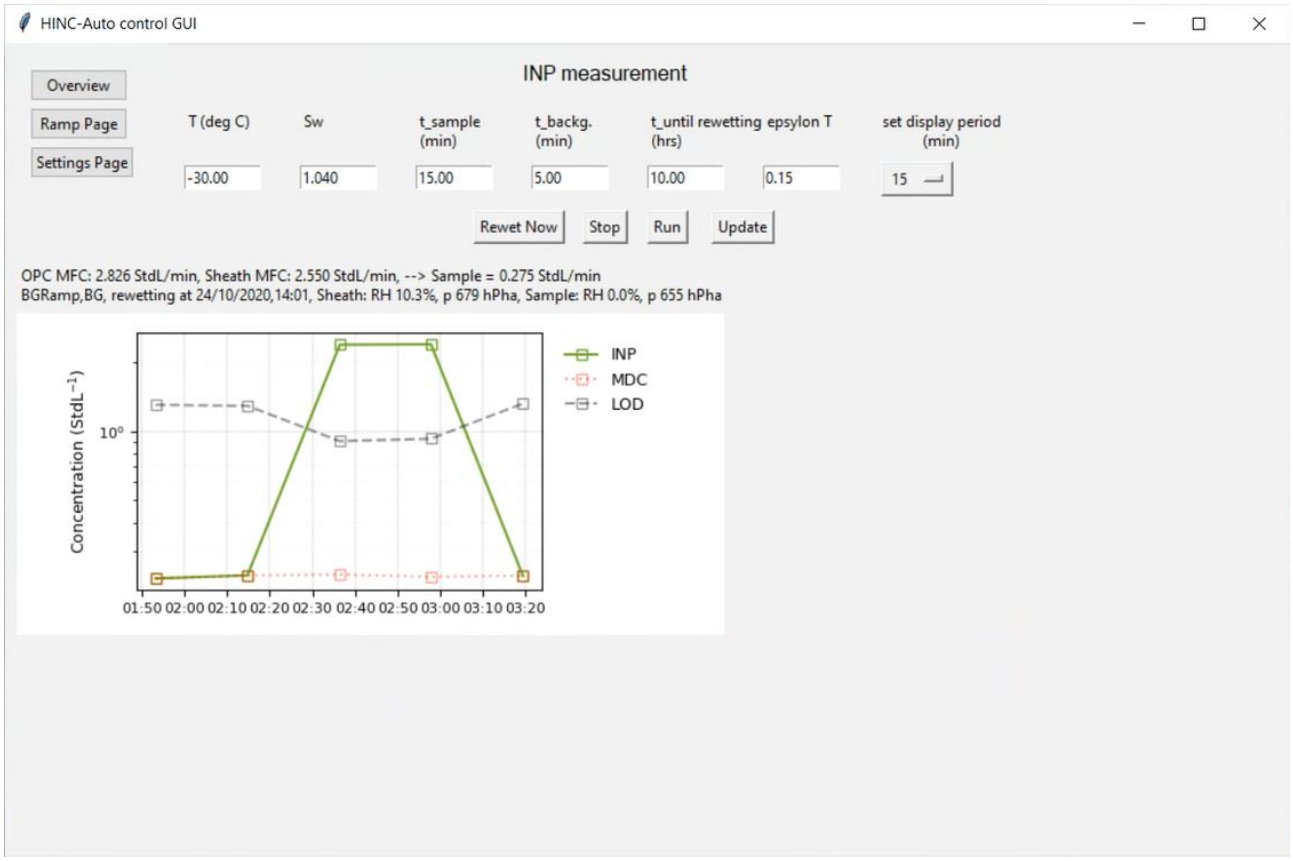

Figure A10. Window of the guided user interface used to control INP measurements with HINC-Auto.

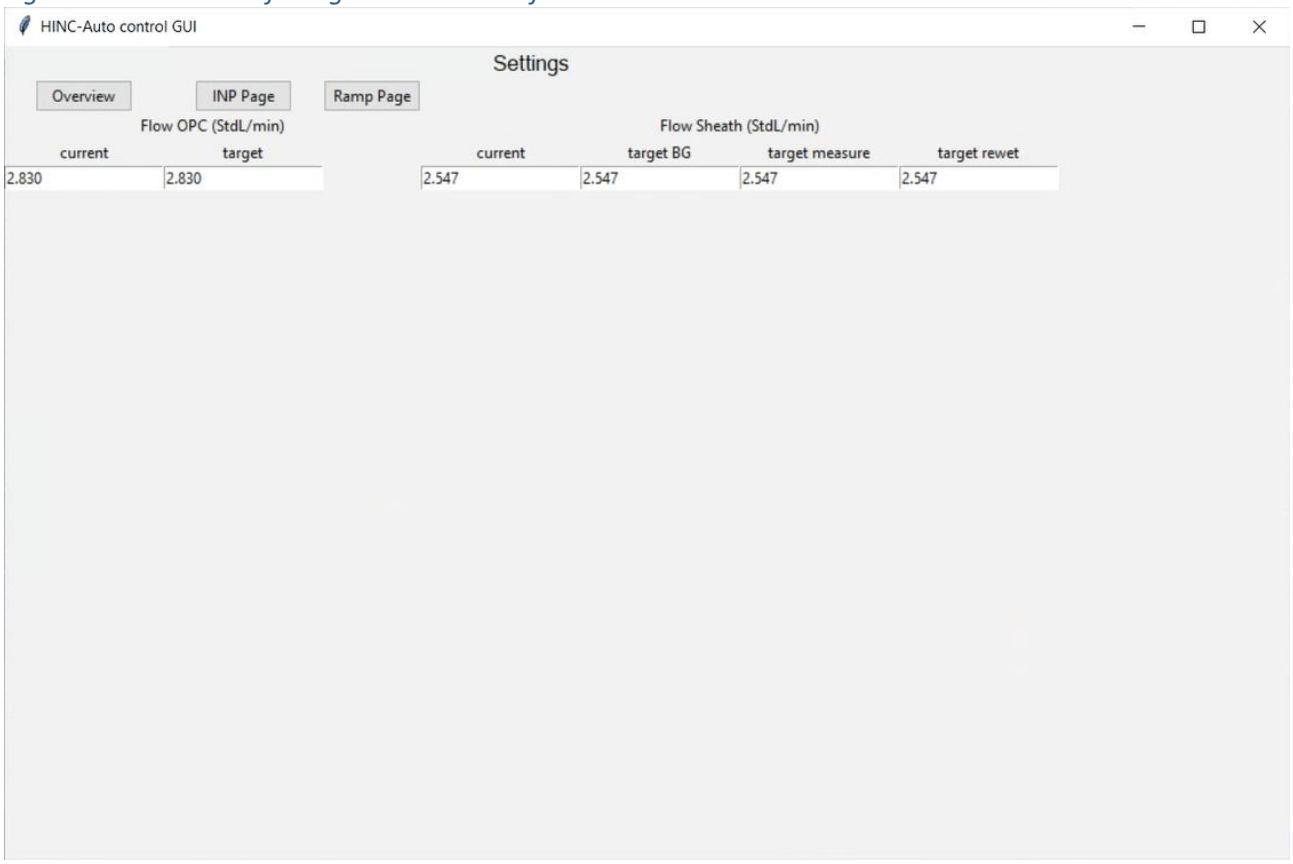

Figure A11. Window of the guided user interface used to adjust additional settings with HINC-Auto.

Line 233: "AF is the ratio of all particles, that are detected in the indicated size bin, to all sampled particles, measured with a CPC within the sample flow." A comment about the smaller particle: The authors discuss about the bigger size of aerosol that can enter HINC auto without being lost due to gravitational loss after activation within HINC-auto. However, what about the other extreme of the particle size distribution, the smaller particle?

We like to thank the reviewer for this important point, since we did not consider commenting on the lower cut-off size of the particles entering the chamber.

What is the (needed) detection limit of the CPC, and why this detection limit was chosen?

The lower the cut-off size is of the CPC the more accurate the ambient aerosol particle counts will be. In the case of the experiments in this work, the CPC has a cut-off size of D50 = 5 nm. This was not actively chosen because for the laboratory measurements we performed experiments with known particles larger tens of nm. The CPC available at the JFJ has a higher size cut-off of D50 = 10 nm. This was also not chosen by us, but it is operated by a different institute under the GAW program.

in other words, is there a minimum size for the particle to enter HINC that could have a chance to activate but not to grow enough to be detected as ice crystal?
For the sampling conditions in HINC (T = 243 K, S_w = 1.04, immersion mode), the smallest particle with the properties of NaCl to be activated would have an initial diameter of 11.4 nm according to Köhler theory. The Kelvin term quickly dominates Köhler theory for these small sizes, thus, a small decrease in initial radius leads to a larger needed increase in activation S_w. Depending on the chemistry of the particle, the initial radius may vary because of the van't Hoff factor or analogous for organic species. If we assume for the solution droplet to immediately freeze after activation it will grow to a diameter of 10.6 µm when having a residence time of 6 seconds in the chamber (diffusional growth by Rogers and Yau (1989)), large enough to be detected by the OPC and differentiated from droplets. We expect that particles with sizes < 12 nm will

therefore not activate into droplets and therefore not freeze, unless they activate by deposition nucleation. Furthermore, we argue that if such particles cannot activate as droplets and freeze by immersion at S_w = 1.04, then they will also not be relevant for ice nucleation in the atmosphere. However, once they coagulate or grow by condensation to sizes larger (> 20 nm) they could activate at lower S_w (< 1.04), which tends closer to atmospherically relevant, at which stage such particles can also activate at our sampling conditions and can be sampled by HINC-Auto. Based on particle loss calculations (von der Weiden et al., 2009) 50% of particles with d = 10 nm and 98% of particles with d = 3 nm are lost in the tubing upstream of the chamber at JFJ.

There is no restriction for small size particle to enter the chamber, would a CPC with very low cutoff size recommended?

A CPC with a very low cutoff point is not necessary in this case because small particles (< 12 nm) would not activate in HINC-Auto, but also not activate in the atmosphere given that S_w > 1.04 would be required as such, these do not need to be counted for estimating atmospherically relevant INP concentrations. Particles smaller than 12 nm resulting from new particle formation (NPF) for example would have to grow by coagulation to become of sizes large enough to activate into droplets and act as INPs in the immersion mode (or in the deposition mode at T < 235 K), however since INP activity scales with surface area, the contributions of particles below 12 nm is not of concern, in fact studies have proposed 100 nm to be the lower size limit for INPs (Pruppacher and Klett, 1997).

Or is there enough small particle loses due to diffusion prior to enter the chamber, in that case what is the cut of size of HINC? or in other word, how can we be sure that all particle that enter HINC and are counted in CPC, can have the possibility to grow big enough to be counted as ice crystal? Can HINC-auto able to measure INP properties of new particle formation that are of size of 5 nm?

In short no, 5 nm particles would need S_w > 1.04 to activate as immersion INPs. So any chamber running at S_w < 1.04 will not be able to account for INPs arising from a 5 nm particle due to Köhler theory limitations, regardless of diffusion losses. However, as we present above, the penetration size of particles into HINC-Auto is 10.3 nm (d_{50}) with 98% of 3 nm particles being lost (particle loss calculator, von der Weiden et al., 2009). Needless to say, all of these scenarios described by the reviewer above would require small particles to grow further to act as INPs even in the atmosphere, as such a 5 nm particle can also not act as an INP in the atmosphere, since it will not activate at atmospherically relevant S_w. So if particles of 5 nm (or less than 12 nm) do not activate in HINC, these will also not activate to droplets and eventually INPs in the atmosphere, unless they grow larger first by coagulation in which case they can be sampled by and activated in HINC-Auto. As such this is not of concern here.

In summary, the losses from diffusion of very small particles entering the tubing are deemed negligible for the measured INP concentration and thus need not be accounted for here. Further, diffusion losses in our laboratory experiments are also considered negligible because we focused on monodisperse particles of 200 nm or polydisperse particles of illite, where particle concentrations below 50 nm are already quite low and not ice-active (Welti et al., 2009) making it a negligible concern for particles below 12 nm.

Fig6a) Why the activated fraction is not 0 at the beginning? is it a real AF or a background of big non activated particle?

We assume the reviewer refers to the high AF in the 0.3 um channel. We believe that the observed ~15% particles above 0.3 µm are due to double (can be up to 25%*) and triple (up to 5.4%*) charged particles when size selecting 200 nm NH_4NO_3 particles (*calculations see Wiedensohler, 1988). A 5-minute background measurement is carried out before and after each ramp, thus at the low and high end of the tested saturation. The background counts are then linearly interpolated between the saturation and subtracted from the counts obtained during the measurement. The non-zero background count can additionally result from large particles that penetrate the DMA due to the transfer function used. In this

particular experiment, we used a lower sheath to sample flow, resulting in a broader transfer function, thus reducing the quality of mono-disperse selection. We now clarify this in the manuscript in line 326.

The sample preparation is as described in section 3.2 for both chambers with a lower DMA sheath flow of 5 L min^{-1} and a higher sample flow of 1.6 L min^{-1} to feed both chambers and the CPC. This resulted in a broader transfer function within the DMA and consequently more larger and multiple charged particles penetrating the size selection. Due to the hygroscopicity of ammonium nitrate, the multiple charged particles are detected in the ≥ 1 µm OPC size bin after hygroscopic growth at S_w < 0.98. In comparison, measurements in section 3.2 and Figure A5 use a narrower DMA transfer function and show a lower activated fraction below S_w < 0.98 than in the experiment with the broader transfer function. The injector position was chosen to result in residence times of τ ≈ 9 seconds.

Fig6a) Why in opc channel >0.3 um there is a small but steady increase of the AF between 0.85 to 0.98 Sw? Is it due to the hygroscopic growth of particle just smaller than 300nm, which with higher humidity grow bigger than 300 nm?

The reviewer's statement is consistent with our understanding of the observed increase in AF. The fraction of size selected particles with a targeted mobility diameter of 200 nm (and double, triple charged particles) that grow because of hygroscopic growth to sizes with an optical diameter of 300 nm or larger increases steadily as the relative humidity is increased from S_w = 0.85 to 0.98.

Line 261: "In either case, the temperature increases in the direction of the air flow, because of the parallel-flow setup of the cooling liquid (see Figure 2b). Therefore, the resulting total temperature variation in the center between the two cooling walls is T ± 0.24 K." I don't understand how the authors get this value of +/-0.24K.

We like to thank the reviewer for pointing out this uncertainty. We aim to clarify by adding figure 7 (revised manuscript):

3.1 Accuracy

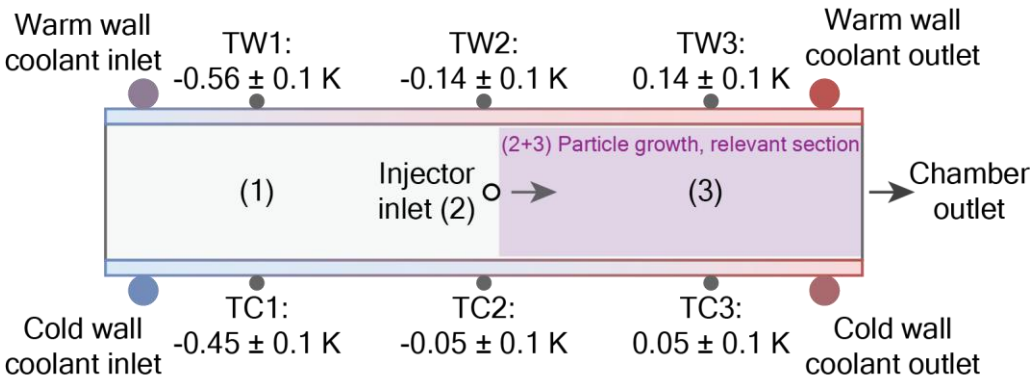

(1): -0.505 ± 0.14 K (2): -0.095 ± 0.14 K (3): 0.095 ± 0.14 K
(2+3): -0.095 - 0.14 to 0.095 + 0.14 K = ±0.24 K

Figure 7. Schematic of uncertainty in temperature measurement showing a side view of HINC-Auto. TW and TC refers to one of six thermocouples installed on the warm wall and cold wall, respectively. Positions (1), (2), (3) and (2+3) indicate the temperature uncertainty of the center lamina. For each of the positions (1), (2), and (3) we have the ± 0.1 K form the warm and ± 0.1 K from the cold wall thermocouple, thus ± $\sqrt{0.1^2 + 0.1^2}$K = ± 0.14.

Four main parameters characterize the INP concentration measured: temperature, supersaturation, particle count and volume flow. The thermocouples have an uncertainty of ± 0.1 K and are calibrated measuring the melting of H_2O and Hg, in close agreement with the ITS-90 (the official protocol of the international

temperature scale). The measured relative (compared to set point T) temperature variation across the warm and cold wall is -0.56/ +0.14 K and -0.45/ +0.05 K at T = 243 K and Sw = 1.04, respectively (see Figure 7). However, on each wall only the two thermocouples close to the injector (TW2/TC2) and the chamber outlet (TW3/TC3) are used to calculate the mean wall temperature. The relative variation therefore decreases to ±0.14 K (at the warm wall) and ±0.05 K (at the cold wall) for a center nominal temperature of T = 243 K at Sw = 1.04. In either case, the temperature increases in the direction of the air flow, because of the parallel-flow setup of the cooling liquid (see Figure 2b). Subsequently, the uncertainty of the center lamina is -0.095 K for the relative variation plus ±0.14 K for the thermocouples uncertainty at location (2) and 0.095 K ± 0.14 K at location (3). Therefore, the resulting total temperature variation in the section relevant for particle nucleation or activation and growth between the two cooling walls is T ±0.24 K. The …

Line 270: "The CPC used for validation experiments has a counting uncertainty of ± 10% which yields in a relative uncertainty in the reported AF of ± 14%" same comment as earlier. how the detection threshold of the CPC affect the AF?

During the validation experiments (subsection 3.2) the sample particles ($(NH_4)_2SO_4$, NaCl, NH_4NO_3) were size selected to a mobility diameter of d_m = 200 nm and in the sedimentation study (Subsection 3.2.2, AgI) to d_m = 100 nm. We believe this should render particles smaller than size cut-off of the CPC used (TSI 3787, D50 = 5 nm) to be negligible contributors to the total particle count. For the INP measurement (Subsection 3.2.3) the NX Illite particles where polydisperse and the SMPS retrieved particle size distribution (Figure 10a) shows more than 4 orders of magnitude lower particle concentrations smaller than 20 nm than between 300 and 500 nm which is substantially below the stated 14% uncertainty in AF. Finally, for the lower size cut-off contribution to field observations please see response to comment about Line 233 above.

Paragraphe 3.2.1: -So here the improvement is due to the flow which is more laminar in HINC-auto, correct? There is no mention of this in the paragraph. -Is this done at particle of size 200 nm? It is not mention in the text.

We agree with the reviewer, and changed the paragraph 3.2.1. as followed:

Figure 8 shows the activation curves of ammonium nitrate size selected to a mobility diameter of d_m = 200 nm and measured at T = 233 K with HINC-Auto compared to measurements performed with HINC. The sample preparation is as described in section 3.2 for both chambers with a lower DMA sheath flow of 5 L min^{-1} and a higher sample flow of 1.6 L min^{-1} to feed both chambers and the CPC. This resulted in a broader transfer function within the DMA and consequently more larger and multiple charged particles penetrating the size selection. Due to the hygroscopicity of ammonium nitrate, the multiple charged particles are detected in the ≥ 1 µm OPC size bin after hygroscopic growth at S_w < 0.98. In comparison, measurements in section 3.2 and Figure A5 use a narrower DMA transfer function and show a lower activated fraction below S_w < 0.98 than in the experiment with the broader transfer function. The injector position was chosen to result in residence times of τ ≈ 9 seconds. The standard sheath to sample flow ratio of HINC-Auto was adjusted to 12:1 to be equal to the ratio used in HINC in order to compare the performance of the two chambers (note that the standard sheath to sample flow ratio of HINC-Auto is 9:1. See section 2.2). HINC-Auto shows an improved precision compared to HINC. We attribute the improvement to the use of the mesh and, subsequently, the more uniform flow within HINC-Auto compared to HINC without the mesh. For measurements in the field with HINC, a defined supersaturation (e.g. S_w = 1.04), temperature and OPC-size bin (e.g. ≥ 4 µm) is used to quantify INPs. Therefore, fluctuations in the activation precision of the ≥ 4 µm size bin can lead to uncertainties in INP concentrations. In the example of HINC, this is equivalent to more than one order of magnitude, thus an improved precision improves the quality of the INP measurements. In addition, particle sedimentation, as expected by theory (see Section below), is visible in the activation curves of HINC-Auto at Sw ≥ 1.02 (see Section 3.2.2).

And if it is monodisperse at 200 nm, why is there an increase of AF bellow 0.975 Sw?

We thank the reviewer for the question. See response to reviewer comment to Fig6a) where we address this concern. Furthermore, we address it in line 326 (revised manuscript).

Line 297: "The sheath to sample flow ratio was 12:1 for both chambers." It was stated Line 267 that the sheath to sample flow ratio should be 9:1. Why is the ratio changed?

The sheath to sample flow ratio of HINC-Auto was adjusted to match the ratio used for the experiments in HINC. This to avoid potential biases when comparing the two chambers (a thinner center lamina results in a steeper activation since the variation in observed temperature and supersaturation is decreased). We added following sentence to Line 297

The standard sheath to sample flow ratio of HINC-Auto was adjusted to 12:1 to be equal to the ratio used in HINC in order to compare the performance of the two chambers (Note that the standard sheath to sample flow ratio of HINC-Auto is 9:1. See section 2.2).

3.2.1 Improvement in precision: Why has –40C been chosen to show the homogeneous freezing onset? At this temperature, the water saturation is very close to the Koop line and it might be hard to distinguish between both. Going lower in temperature would show two distinct activation points.

We agree with the reviewer, for the performance of homogeneous freezing onset, we refer readers to Figure 7 (and Figure A5), where we show experiments below 233 K. The key message of Section 3.2.1 and intended with Figure 8 is to demonstrate the precision increased with HINC-Auto compared to HINC when running multiple experiments.

Line 356: "The for the initial scan (solid line) the sheath flow set to 5 L min−1, and for the second scan to 2 L min−1 (dashed line)." please correct. Also, authors could state that at lower sheath flow, SMPS covers bigger particle size while losing smaller particle size.

We agree with the reviewer, and changed Line 356 as followed:

~~The~~ *For the initial scan (solid line) the sheath flow was set to 5 L min-1, and for the second scan to 2 L min-1 (dashed line). At a lower sheath flow rate, the SMPS scan shifts to cover a larger range of particle sizes while limiting the scanning range at smaller particle sizes.*

Line 359: "This is contradicting our assumption and the lower sheath flow rate of the DMA for the second compared to the first measurement could be the reason." Could it be that with different sheath flow rates, the author can measure at different size range? And also during the time in the stainless steel chamber, coagulation of particle could have made the particles to grow bigger.

We agree with the input of the reviewer about coagulation, and changed Line 359 as followed:

This contradicts our initial assumption of large particles sedimenting more quickly than small particles, thus shifting size distribution towards smaller particle sizes with time. A reason could be due to particle coagulation in the stainless steel aerosol chamber, which causes the observed shift in size distribution towards larger particle sizes.

Line 364: "For atmospheric relevant conditions at the JFJ with 400 cm−3 ≤ N ≤ 1000 cm−3 the drop occurs after 8.5 hours, for 95 cm−3 ≤ N ≤ 200 cm−3 after 13 hours."
- how the authors define the drop? (drop of 20%?) -while the data agree with authors statement (data started at 25/12 and at almost 26/12), later in the experiment, after time 2, the data seems to suggest a need of more frequent rewetting. especially the experiment just after "time 2" and the next one.

The reviewer is correct in asking how we define a drop. Since the drop is gradual, it is not possible to have a stringent cutoff (like 20 or 30%). However, motivated by the reviewer comment we agree that a more

frequent rewetting should be implemented. We now choose to be more conservative and use the drop observed after 8.5 hours as the re-wetting time. As such we now adjust the recommendation to 8 hours for re-wetting and have also adjusted this for the ongoing field measurements (see website). We changed the following sentence Line 369 (initial manuscript) to

Based on the above experiment we choose a rewetting time of 8 hours for field applications in remote areas such as Jungfraujoch.

Line 369: "Based on the above experiment, we chose a rewetting time of 10 hours for field applications (Section 3.3)." As the rewetting is automatic and fast, why not choosing a more frequent rewetting to ensure good data, (i.e. to be on the safe side)?

We agree with the reviewer. We initially choose to do the rewetting sequence less often because of two reasons:

1. The (mechanical/ thermal) stress on the chamber is largest during the rewetting procedure. Frequent rewetting reduces the lifetime of the components and could increase probability of breakdown.
2. If data is acquired over a long period of several months, analysis of the data with subsequent filtering is possible. Because of the large amount of data, ideally will not compromise the quality of the results drastically. The time between two rewetting procedures can then be adapted (which we now do and changed to 8 hours).

Or did the author choose a 10 hours rewetting interval because at higher altitude, residence time is shorter, and in result the water depletion is longer?

No, although we support the reviewer's statement, we did not think of this when choosing the rewetting interval. The rewetting time has now been changed to 8 hours.

Line 378: "Design changes implemented in a second field campaign started in February 2020 resulted in a median LOD of 1.37 std L−1" Could the author specify which design change has been made, which allows a decrease by factor of almost 3 of the LOD? This would be very valuable for the INP community.

We agree with the comment of the reviewer and changed Line 378 as followed:

Design changes implemented in a second field campaign started in February 2020 resulted in a median LOD of 1.37 std L^{-1}. It was observed that ice crystals and frost deposited within the cavity of the chamber outlet. We assumed for supercooled liquid droplets, which make up the majority of the hydrometeor population exiting the chamber, to impact on the surfaces where the Swagelok fitting (to connect the OPC) is inserted into the PVDF frame. The change in inner diameter from the cavity within the PVDF frame (d_i = 10.2 mm) to the fitting (d_i = 3.3 mm) is like a step. The design changes included using a conical drill bit (20°) to smoothen the connection between the chamber outlet and the fitting. In addition, the Swagelok fitting is warmed with a 10 W heat pad during the rewetting procedure to support the evaporation of residual condensate or molten ice that does not drain due to gravity while the chamber is tilted.

Typo: caption fig 8: "with identical particle residence times. of" remove "."

We changed the caption of Figure 8 as proposed by the reviewer. Thanks for catching that.

References

Bi, K., McMeeking, G. R., Ding, D. P., Levin, E. J., DeMott, P. J., Zhao, D. L., Wang, F., Liu, Q., Tian, P., Ma, X. C., Chen, Y. B., Huang, M. Y., Zhang, H. L., Gordon, T. D., and Chen, P.: Measurements of Ice Nucleating Particles

in Beijing, China, Journal of Geophysical Research: Atmospheres, 124, 8065–8075, https://doi.org/https://doi.org/10.1029/2019JD030609, 2019.

Kunert, A. T., Pöhlker, M. L., Tang, K., Krevert, C. S., Wieder, C., Speth, K. R., Hanson, L. E., Morris, C. E., Schmale, D. G., Pöschl, U., and Fröhlich-Nowoisky, J.: Macromolecular fungal ice nuclei in Fusarium: effects of physical and chemical processing, Biogeosciences, 16, 4647–4659, https://doi.org/https://doi.org/10.5194/bg-16-4647-2019, 2019.

Möhler, O., Adams, M., Lacher, L., Vogel, F., Nadolny, J., Ullrich, R., Boffo, C., Pfeuffer, T., Hobl, A., Weiß, M., Vepuri, H., Hiranuma, N., and Murray, B.: The portable ice nucleation experiment PINE: a new online instrument for laboratory studies and automated long-term field observations of ice-nucleating particles, Atmospheric Measurement Techniques Discussions, pp. 1–43, https://doi.org/https://doi.org/10.5194/amt-2020-307, in review, 2020.

Pruppacher, H. and Klett, J.: Microphysics of Clouds and Precipitation, Springer Netherlands, 2 edn., https://doi.org/https://doi.org/10.1007/978-0-306-48100-0, 1997.

Rogers, R. R. and Yau, M. K.: A short course in cloud physics / R. R. Rogers and M. K. Yau, Oxford, Pergamon Press. Rosenfeld, 3, illustrated, reprint edn., 1989.

Von der Weiden, S.-L., Drewnick, F., and Borrmann, S.: Particle Loss Calculator – a new software tool for the assessment of the performance of aerosol inlet systems, 2, 479–494, https://doi.org/https://doi.org/10.5194/amt-2-479-2009, 2009.

Welti, A., Lüönd, F., Stetzer, O., and Lohmann, U.: Influence of particle size on the ice nucleating ability of mineral dusts, Atmospheric Chemistry and Physics, 9, 6705–6715, https://doi.org/10.5194/acp-9-6705-2009, 2009.